Lack of Vitamin D Receptor Leads to Hyperfunction of Claudin-2 in Intestinal Inflammatory Responses

Yong-guo Zhang, PhD,[*] Rong Lu, MD, PhD,[*] Yinglin Xia, PhD,[*] David Zhou, MD, PhD,[†,‡] Elaine Petrof, MD,[§] Erika C. Claud, MD,[¶] and Jun Sun, PhD,[*]

Background: Vitamin D3 and vitamin D receptor (VDR) are involved in the pathogenesis of inflammatory bowel disease (IBD) and bacterial infection. Claudin-2 is a junction protein that mediates paracellular water transport in epithelia. Elevation of Claudin-2 is associated with active IBD. However, VDR involved in epithelial junctions under inflammation and infection remains largely unknown. We investigated the mechanisms on how VDR and Claudin-2 are related in inflamed states.

Methods: Using cultured VDR$^{-/-}$ enteroids, human intestinal epithelial cells, VDR$^{-/-}$ mice with *Salmonella*- or DSS-colitis, and human IBD samples, we investigated the mechanisms how VDR and Claudin-2 are related in inflamed states.

Results: After *Salmonella* infection had taken place, we observed significantly enhanced Claudin-2 and an increased bacterial invasion and translocation. A lack of VDR regulation led to a robust increase of Claudin-2 at the mRNA and protein levels post-infection. In DSS-treated VDR$^{-/-}$ mice, Claudin-2 was significantly increased. Location and quantification of Claudin-2 protein in the mouse colons treated with DSS also confirmed these results. Inflammatory cytokines were significantly higher in the serum and mRNA levels in intestine, which are known to increase Claudin-2. Furthermore, in inflamed intestine of ulcerative colitis patients, VDR expression was low and Claudin-2 was enhanced. Mechanistically, we identified the enhanced Claudin-2 promoter activity through the binding sites of NF-κB and STAT in inflamed VDR$^{-/-}$ cells.

Conclusions: Our studies have identified a new role for intestinal epithelial VDR in regulating barrier functions in the context of infection and inflammation.

Key Words: Claudin-2, inflammation, intestine, nuclear factor kappa-light-chain-enhancer of activated B cells (NF-κB), signal transducer and activator of transcription (STAT), STAT3, organoids, permeability, tight junction, vitamin D, vitamin D receptor

INTRODUCTION

Tissue barrier functions are determined by tight junction (TJ) structural components.[1–6] Defective intestinal barrier function has been implicated in inflammatory bowel disease (IBD) and can predict relapse during clinical remission.[7] Claudin-2 forms a water channel to permit the paracellular passage of water through its pore in epithelia.[8] Colonic Claudin-2 expression is uniquely restricted to the crypt base, which is the proliferative zone.[9, 10] Increased Claudin-2 tends to make intestinal epithelial cells leakier.[7, 10–17] Elevation of Claudin-2 is associated with active human IBD.[18, 19]

Impaired epithelial barriers are not only associated with chronic inflammation but also infection. *Salmonella enterica* serotypes are invasive enteric pathogens spread through fecal contamination of food and water sources. *Salmonella* induce the disruption of intestinal barriers during infection.[20–24] Our previous study has demonstrated that *Salmonella* manipulate the distribution of Claudin-2 and elevated its protein expression in intestine.[24] Intestinal epithelial cells with Claudin-2 knockdown had significantly less internalized *Salmonella* than control cells with normal Claudin-2 expression.[24]

The nuclear vitamin D receptor (VDR) mediates most known functions of 1,25-dihydroxyvitamin D. Vitamin D and VDR are key players in calcium homeostasis.[25] It also plays a protective role in infection and inflammation.[26, 27] Vitamin D deficiency has been implicated in patients with IBD.[28–32] Vitamin D receptor is identified as an IBD risky gene.[33–37] Tight junction proteins (eg, ZO-1 and Occludin) are known to maintain a barrier.[38] ZO-1 and Occludin are upregulated in intestinal epithelial cells by 1,25 $(OH)_2D_3$ treatment in vitro.[39, 40] Claudin-2 has been identified as a target gene of the VDR

Received for publications April 18, 2018; Editorial Decision August 23, 2018.

From the *Department of Medicine, University of Illinois at Chicago, Chicago, Illinois, USA; †Department of Pathology, University of Rochester, Rochester, New York, USA; ‡Department of Pathology and Immunology, Washington University in St. Louis, St. Louis, Missouri, USA; §Department of Medicine, GI Diseases Research Unit and Division of Infectious Diseases, Queen's University, Kingston, Ontario, Canada; ¶Departments of Pediatrics and Medicine, The University of Chicago, Chicago, Illinois, USA

Author contributions: YZ, RL, and YX contributed to the acquisition, analysis and interpretation of data, drafting the manuscript, and statistical analysis. DZ, EP, and ECC contributed to technical or material support and drafting the manuscript. JS contributed to the study concept and design, obtaining funding, supervising the study, analysis and interpretation of data, and writing the manuscript.

Supported by the NIDDK/National Institutes of Health grants R01 DK105118, R01DK114126, and DOD BC160450P1 given to JS.

Address correspondence to: Jun Sun, PhD, AGA Fellow, Professor Division of Gastroenterology and Hepatology Department of Medicine, University of Illinois at Chicago 840 S. Wood Street, Room 704 CSB, MC716 Chicago, IL, 60612, USA. E-mail: junsun7@uic.edu

doi: 10.1093/ibd/izy292
Published online 4 October 2018

signaling in cells without any inflammatory stimulation.[41, 42] Therefore, it is interesting to study how VDR is involved in regulating Claudin-2 and barrier functions under inflammation and infection. Insights into the mechanisms responsible for VDR and intestinal barrier dysfunction are needed, especially in disease models in vivo.

In the current study, we hypothesize that a lack of intestinal VDR leads to hyperfunction of Claudin-2 and impaired barrier functions in infection and inflammatory responses. Using $VDR^{-/-}$ mice, organoids, human samples, and cultured human intestinal epithelial cells, we performed a series of molecular and biochemical experiments in vivo and in vitro to investigate VDR regulation of Claudin-2 expression in infection and inflammation. We investigated the mechanisms on how VDR and Claudin-2 are related in inflamed states. Our findings reveal a novel role of VDR in regulating barrier functions in inflammation and infectious disease.

MATERIALS AND METHODS

Human Tissue Samples

This study was performed in accordance with approval from the University of Rochester Ethics Committee (RSRB00037178). Colorectal tissue samples were obtained with informed consent from the sigmoid colon of patients exhibiting no apparent intestinal pathology and from the mucosa of patients undergoing anterior resection. All pathologic diagnoses were evaluated by pathologists. The ulcerative colitis (UC) cohort consisted of 16 patients with previous diagnosis of UC (10 female, 6 male, mean age = 66.6 years, range of 51 to 83), while the age-matched control cohort consists of 10 patients (6 female, 4 male, mean age = 65.7 years, range of 44 to 85) without previous diseases in gastrointestinal tract. All patient samples were obtained at the University of Rochester Medical Center from 2008 to 2012. In this study, no Crohn's disease (CD) patients were included.

Animals

$VDR^{+/-}$ and $VDR^{-/-}$ mice on a C57BL6 background were obtained by breeding heterozygous $VDR^{+/-}$ mice.[43] $VDR^{+/-}$ and $VDR^{-/-}$ mice were used to compare the difference between VDR-null and 1 allele of the VDR gene. We also confirmed similar results were obtained when $VDR^{+/+}$ mice were used (data not shown). Mice were fed a normal chow diet and under 12:12 light/dark cycles. Experiments were performed on 2 to 3 months old mice. The animal work was approved by the UIC Office of Animal Care and the Rush University Committee on Animal Resources. Euthanasia method was sodium pentobarbital (100 mg per kg body weight) intraperitoneal (IP) injection, followed by cervical dislocation. All experiments were carried out in accordance with the approved guidelines.

Culture of Mouse Small Intestinal Organoids and Treatment With *Salmonella*

Organoids from small intestine of $VDR^{+/-}$and $VDR^{-/-}$ mice were prepared and maintained as previously described.[44, 45] Mini gut medium [advanced Dulbecco's Modified Eagle's Medium (DMEM)/F12 supplemented with HEPES, L-glutamine, N2, and B27] was added to the culture, along with R-Spondin, Noggin, and epidermal growth factor (EGF). At day 7 after passage, organoids were colonized by *Salmonella* for 30 minutes, then washed, and incubated for 1 hour in Mini gut medium with Gentamicin (500 µg/mL).

Bacterial Strains and Growth Condition

Wild-type *Salmonella* Typhimurium ATCC14028 was used in this study. Nonagitated microaerophilic bacterial cultures were prepared.[46]

Streptomycin Pretreated Mouse Model

Animal experiments were performed using specific-pathogen-free female $VDR^{+/-}$ and $VDR^{-/-}$ mice that were 6 to 8 weeks old, as previously described.[47] Water and food were withdrawn 4 hours before oral gavage with 7.5 mg/mouse of streptomycin (100 µL of sterile solution or 100 µL of sterile water in control). Afterward, animals were supplied with water and food ad libitum. Twenty hours after streptomycin treatment, water and food were withdrawn again for 4 hours before the mice were infected with $1x10^7$ CFU of *S. typhimurium* [100 µL suspension in Hank's Balanced Salt Solution (HBSS)] or treated with sterile HBSS (control). Three days after infection, mice were sacrificed, and tissue samples from the intestinal tracts were removed for analysis.

Salmonella Burden in Intestine, Spleen, and Liver

Intestine, liver, and spleen were dissected from each mouse, put into 14-mL tubes with 5 mL of sterile phosphate-buffered saline (PBS), cut into pieces with scissors, then homogenized adequately using a Polytron PT2100 (Kinematica, Switzerland). Each homogenate was diluted 1000× to 10,000× with Luria Broth (LB), plated (100 µL) on MacConkey agar plates, and incubated at 37°C overnight. Colony-forming units were quantified.

Induction of Mouse Colitis and Assessment of Clinical Disease

Mice were fed 3% (wt/vol) dextran sulfate sodium (DSS, molecular mass = 36 to 50 kD; USB Corp. Cleveland, OH, USA) dissolved in filter-purified and sterilized water.[48] At day 3 after DSS administration, mice were scarified. Body weight and animal symptoms, including the extent of diarrhea and rectal bleeding, were closely monitored during and after DSS treatment. Symptom scores were determined by assessing the degree of body weight loss, stool consistency (diarrhea), and

hemoccult positivity or gross blooding in each animal according to previously published methods.[40]

Histology

For each animal, histological examination was performed of the cecum. Cecum length and inflammation were key features in this *Salmonella*-colitis mouse model.[49] Cecum length was measured using a ruler. Histological parameters were quantified in a blinded fashion using modified validated scoring systems.[48–50] Six independent parameters were measured: severity of inflammation, depth of injury, crypt damage, submucosal edema, polymorphonuclear cells (PMNs) in the lamina propria, and mean number of goblet cells. Histological scores were multiplied by a factor reflecting the percentage of tissue involvement (×1, 0%–25%; ×2, 26%–50%; ×3, 51%–75%; ×4, 76%–100%), and values were added to obtain a total score.

Cell Culture

Human epithelial CaCO2 and SKCO15 cells were maintained on transwell inserts (0.33 or 4.67 cm^2, 0.4 mm pore; Costar, Cambridge, MA, USA) in DMEM supplemented with 10% fetal bovine serum, penicillin-streptomycin (Penicillin, 100 I.U./mL/Streptomycin, 100µg/mL), and L-glutamine (4.5g/L). Human epithelial HCT116 cells, $VDR^{+/-}$ mouse embryonic fibroblasts (MEF), and $VDR^{-/-}$ MEF cells were cultured in DMEM medium supplemented with 10% (vol/vol) fetal bovine serum, as previously described.[52, 53]

Immunoblotting

Cultured cells were rinsed twice with ice-cold HBSS, lysed in protein-loading buffer (50 mM Tris, pH 6.8, 100 mM dithiothreitol, 2% SDS, 0.1% bromophenol blue, 10% glycerol), and then sonicated. Mouse colonic epithelial cells were collected by scraping the tissue from the colon of the mouse, including the proximal and distal regions.[51, 52] The cells were sonicated in lysis buffer [10 mM Tris, pH 7.4, 150 mM NaCl, 1 mM ethylene diamine tetraacetic acid (EDTA), 1 mM ethylene glycol tetraacetic acid (EGTA), pH 8.0, 1% Triton X-100] with 0.2 mM sodium ortho-vanadate, and protease inhibitor cocktail. The protein concentration was measured using the BioRad Reagent (BioRad, Hercules, CA, USA). Equal amounts of protein were separated by SDS-polyacrylamide gel electrophoresis, transferred to nitrocellulose, and immunoblotted with primary antibodies. The following antibodies were used: anti-claudin-2, anti-claudin-3, anti-claudin-7 (Invitrogen, Carlsbad, CA, USA), anti-p-STAT3, anti-STAT3, anti-p-IκBα, anti-IκBα, anti-p-SAPK/JNK, anti-SAPK/JNK (Cell Signal, Beverly, MA, USA), anti-Villin, and anti-VDR (Santa Cruz Biotechnology Inc., Santa Cruz, CA, USA), or anti-β-actin (Sigma-Aldrich, Milwaukee, WI, USA) antibodies and were visualized by enhanced chemiluminescence (ECL). Membranes that were probed with more than one antibody were stripped before reprobing.

Immunofluorescence

Colonic tissues were freshly isolated and embedded in paraffin wax after fixation with 10% neutral buffered formalin. Immunofluorescence was performed on paraffin-embedded sections (4 µm), after preparation of the slides as described previously,[53] followed by incubation for 1 hour in blocking solution (2% bovine serum albumin, 1% goat serum in HBSS) to reduce nonspecific background. The tissue samples were incubated overnight with primary antibodies at 4°C. The following antibodies were used: anti-Claudin-2, anti-Claudin-7 (Invitrogen, Grand Island, NY, USA), anti-*Salmonella* t*yphimurium* (Santa Cruz Biotechnology Inc., Santa Cruz, CA, USA). Samples were then incubated with secondary antibodies (goat anti-mouse Alexa Fluor 488 or goat anti-rabbit Alexa Fluor 488, Molecular Probes, CA; 1:200) for 1 hour at room temperature. Tissues were mounted with SlowFade Antifade Kit (Life technologies, s2828, Grand Island, NY, USA), followed by a coverslip, and the edges were sealed to prevent drying. Specimens were examined with a Zeiss laser scanning microscope (LSM 710 (Carl Zeiss Inc., Oberkochen, Germany).

Vitamin D Receptor and Claudin-2 Expression in Human IBD

Immunohistochemistry (IHC) of VDR and immunofluorescence (IF) of Claudin-2 in human normal and ulcerative colitis samples staining were scored by a well-trained pathologist. Immunohistochemistry of VDR and IF of Claudin-2 staining was initially assessed as a product of staining intensity (0, no staining; 1, minimal; 2, slight; 3, moderate; 4, marked intensity). We randomly took 3 scores derived from each samples. As a result, the final analytical sample consisted of 30 normal scores and 48 UC scores.[54] Statistical analyses were performed using Student *t* test.

In Vivo Permeability Measurements Across Colonic Mucosa

Mice were treated with *Salmonella* for 3 days. Fluorescein Dextran (Sigma-Aldrich, St. Louis, MO, USA; Molecular weight 3000 Da, diluted in HBSS) was gavaged (50 mg/g mouse). Four hours later, mouse blood samples were collected for fluorescence intensity measurement.[23]

Mouse Cytokine

Mouse blood samples were collected by cardiac puncture and placed in tubes containing EDTA (10 mg/mL). Mouse cytokines were measured using a mouse cytokine 10-Plex Panel kit (Invitrogen, Carlsbad, CA, USA) according to the manufacturer's instructions. Briefly, beads of defined spectral properties were conjugated to protein-specific capture antibodies and added along with samples (including standards of known protein concentration, control samples, and test samples) into

the wells of a filter-bottom microplate, where proteins bound to the capture antibodies over the course of a 2-hour incubation. After washing the beads, protein-specific biotinylated detector antibodies were added and incubated with the beads for 1 hour. After removal of excess biotinylated detector antibodies, the streptavidin-conjugated fluorescent protein R-phycoerythrin (streptavidin-RPE) was added and allowed to incubate for 30 minutes. After washing to remove unbound streptavidin-RPE, the beads were analyzed with the Luminex detection system PerkinElmer CS1000 Autoplex Analyzer (PerkinElmer Inc., Waltham, MA, USA).

Transient Transfections

Transient transfections were performed with Lipofectamine 2000 (Invitrogen, San Diego, CA, USA) in accordance with the manufacturer's instructions. Cells were seeded on 60-mm dishes overnight before transfection with plasmids. Plasmid DNA solution was mixed with the transfection reagent at a ratio of 1:1 before being added to cells. After a 24-hour transfection period, the proteins were extracted for analysis.

Vitamin D Receptor siRNA

SKCO15 cells were grown in 12-well plates. The cells were transfected with on-Target plus smart pool human VDR siRNA (Dharmacon Inc., Lafayette, MO, USA) or scrambled siRNA control (Santa Cruz Biotechnology Inc., Santa Cruz, CA, USA) using Surefect reagent (SABiosciences, Frederick, MD, USA). After 72-hour transfection, cells were colonized by *Salmonella* for 30 minutes, then washed and incubated in DMEM with Gentamicin (500 μg/mL) within the indicated time.

Transcriptional Activation

Deletions of different domains of the Claudin-2 promoter plasmids were constructed as previously described.[41] After a 24-hour transfection period, cells were colonized by *Salmonella* for 30 minutes, washed, and incubated for 30 minutes in DMEM with Gentamicin (500 μg/mL). The cells were lysed, and luciferase activity was determined using the Dual Luciferase Reporter Assay System (Promega, Madison, WI, USA) with a TD-20/20 luminometer (Turner Designs, Sunnyvale, CA, USA). Firefly luciferase activity was normalized to *Renilla* luminescence activity, and the activity was expressed as relative units.

Real-Time Quantitative Polymerase Chain Reaction Analysis

Total RNA was extracted from mouse epithelial cells or cultured cells using TRIzol reagent (Invitrogen, Grand Island, NY, USA). The RNA integrity was verified by electrophoresis. RNA reverse transcription was performed using the iScript cDNA synthesis kit (Bio-Rad, Hercules, CA, USA) according to the manufacturer's protocol. The RT cDNA reaction products were subjected to quantitative real-time polymerase chain reaction (RT-PCR) using CTFX 96 Real-time system (Bio-Rad, Hercules, CA, USA) and SYBR green supermix (Bio-Rad, Hercules, CA, USA) according to the manufacturer's protocol. All expression levels were normalized to β-actin levels of the same sample. Percent expression was calculated as the ratio of the normalized value of each sample to that of the corresponding untreated control cells. All real-time PCR reactions were performed in triplicate. Optimal primer sequences were designed using Primer-BLAST or were obtained from Primer Bank primer pairs listed in Table 1.

TABLE 1. Real-time PCR Primers

Primers name	Sequence
mβ-actinF	5′-TGTTACCAACTGGGACGACA-3′
mβ-actinR	5′-CTGGGTCATCTTTTCACGGT-3′
mVDRF	5′-GAATGTGCCTCGGATCTGTGG-3′
mVDRR	5′-ATGCGGCAATCTCCATTGAAG-3′
mClaudin-2F	5′-GCAAACAGGCTCCGAAGATACT-3′
mClaudin-2R	5′-GAGATGATGCCCAAGTACAGAG-3′
mTNF-αF	5′-CCCTCACACTCAGATCATCTTCT-3′
mTNF-αR	5′-GCTACGACGTGGGCTACAG-3′
mIL-6-F	CTGCAAGAGACTTCCATCCAG
mIL-6-R	AGTGGTATAGACAGGTCTGTTGG

Statistical Analysis

All data are expressed as the mean ± SD. All statistical tests were 2-sided. All P values <0.05 were considered statistically significant. The distribution of each outcome variable was tested before statistical analysis. The test results showed that the outcome data are normally distributed. Thus, the differences between samples were analyzed using Student t test for 2 groups and using 1-way ANOVA for more than 2 groups, respectively. Multiple comparisons of mean body weight were performed using 2-way ANOVA. Because we were interested in comparing the mean differences among treatment groups, the group effects at each post-treatment days of 1, 2, and 3 were tested using generalized linear mixed models. The P values in ANOVA analysis and generalized linear mixed models were adjusted using the Tukey method to ensure accurate results. Statistical analyses were performed using SAS version 9.4 (SAS Institute, Inc., Cary, NC, USA).

RESULTS

Claudin-2 Protein Was Significantly Increased in *Salmonella*-Colonized VDR$^{-/-}$ Cells

We have reported a *Salmonella*-infected organoid culture system suitable for studying host-bacterial interactions.[55] We used the VDR$^{+/-}$ and VDR$^{-/-}$ organoids infected with

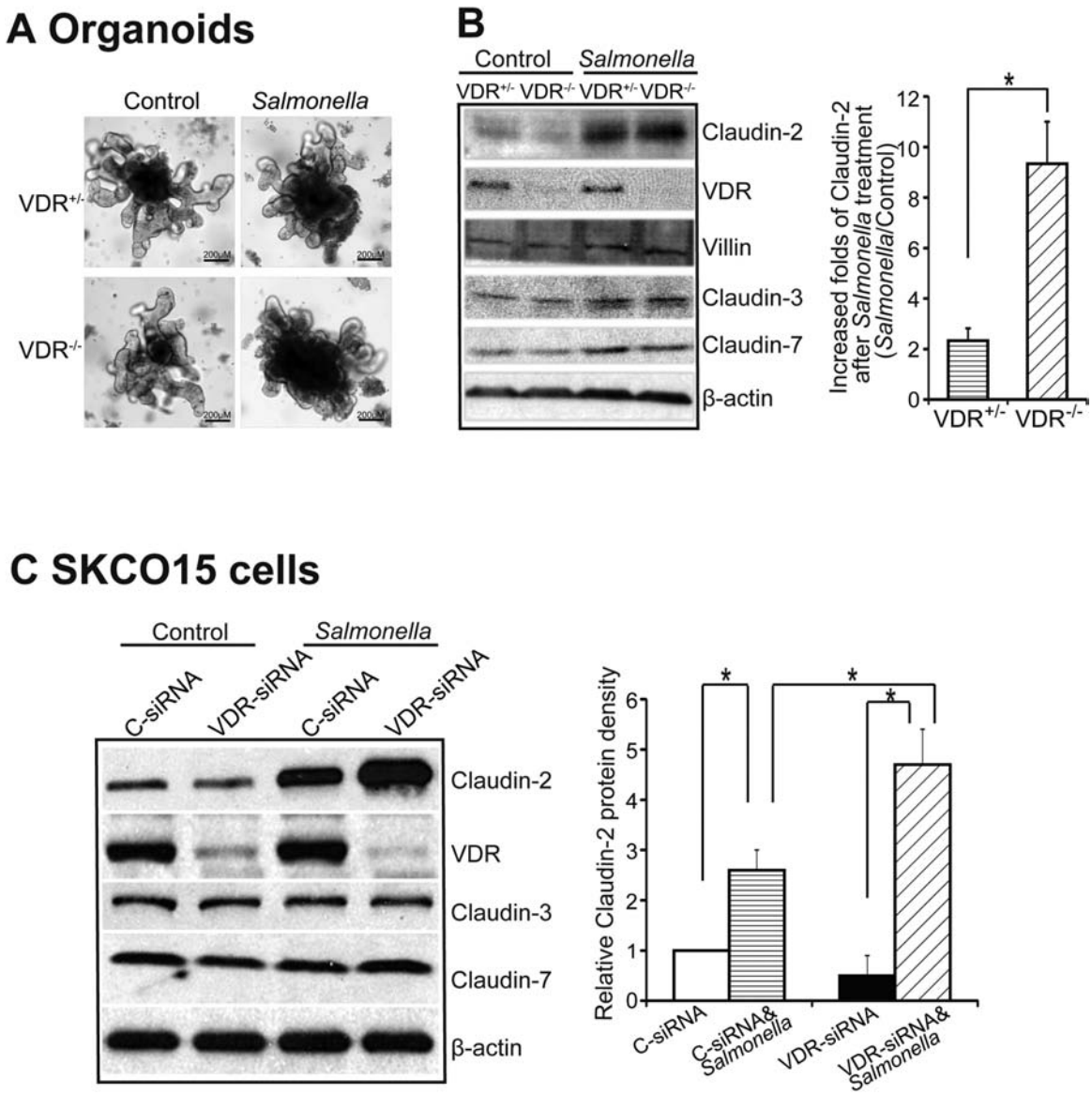

FIGURE 1. Claudin-2 protein expression was significantly increased in *Salmonella*-colonized VDR$^{-/-}$ cells. A, The micrographs showed representative VDR$^{+/-}$ and VDR$^{-/-}$ organoids with or without *Salmonella* infection. Each condition was examined in triplicates with multiple (>10) organoids in each sample. Each experiment was repeated three times. B, Claudin-2 protein expression increased 9.3-fold in VDR$^{-/-}$ organoids and 2.3-fold in VDR$^{+/-}$ organoids infected with *Salmonella* compared with control. (Data are expressed as mean ± SD; n = 3, Student *t* test, **P* < 0.05). C, Claudin-2 protein expression was upregulated in VDR-siRNA SKCO15 cells compared with C-siRNA SKCO15 cells infected with *Salmonella*. SKCO15 cells were transfected with human VDR siRNA or scrambled siRNA control according to the manufacturer's instructions. At 72 hours post-transfection, cells were colonized by *Salmonella* for 30 minutes, washed, and incubated for 30 minutes in DMEM with Gentamicin (500 μg/mL). Cell lysis samples were collected for western blots. (Data are expressed as mean ± SD; n = 3, 1-way ANOVA test; **P* < 0.05).

Salmonella (Fig. 1A). Vitamin D receptor protein level was lower in the VDR$^{-/-}$ organoids at the basal level. *Salmonella* infection induced significantly higher Claudin-2 upregulation in the VDR$^{-/-}$ organoids compared with the VDR$^{+/-}$ organoids with normal level of VDR (Fig. 1B). In the loss function study, we knocked down VDR in human SKCO15 cells using VDR-siRNA. We found that cells with lower VDR expression had higher Claudin-2 upregulation after *Salmonella* infection compared with the cells with normal level of VDR (Fig. 1C). Overall, these data indicate that a lack of VDR leads to a robust increase of Claudin-2 post *Salmonella* infection.

More Severe *Salmonella*-Infection in the VDR$^{-/-}$ Mice

Based on the in vitro data in Fig. 1, we further hypothesize that infection and inflammation may take over and drive

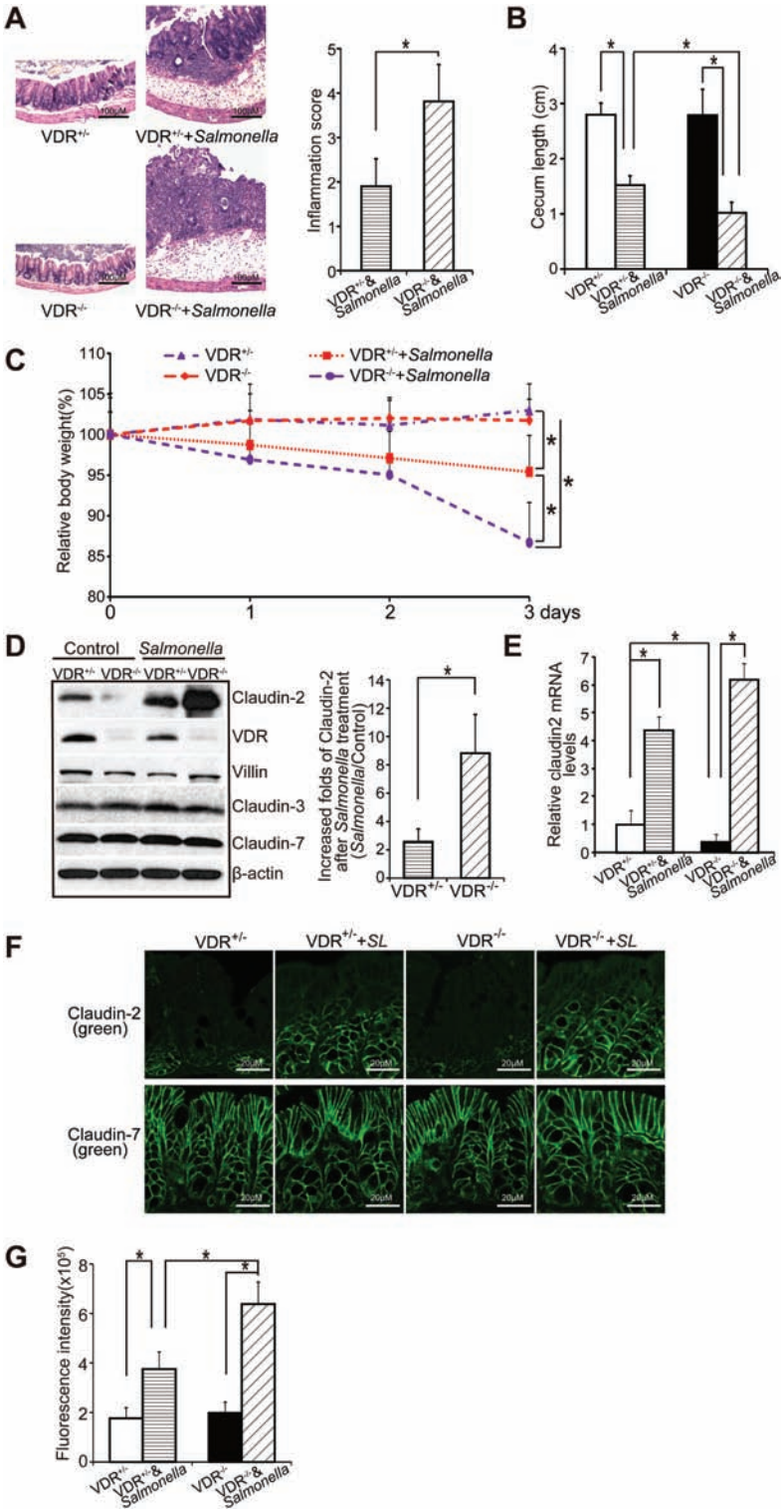

FIGURE 2. VDR$^{-/-}$ mice were more susceptible to *Salmonella* infection than VDR$^{+/-}$ mice. A, Representative H&E staining and inflammation scores of intestine tissues from VDR$^{+/-}$ and VDR$^{-/-}$ mice with or without *Salmonella* infection. (Data are expressed as mean ± SD; n = 7 mice/group, 1-way ANOVA test; *$P < 0.05$). B, Cecum shortening was observed in the VDR$^{-/-}$ mice infected with *Salmonella*. The cecum length was significantly shorter in the VDR$^{-/-}$ mice infected with *Salmonella* compared with the VDR$^{+/-}$ mice infected with *Salmonella*. (Data are expressed as mean ± SD; n = 7 mice/group, 1-way ANOVA test; *$P < 0.05$.) C, Relative body weight changes in VDR$^{+/-}$ and VDR$^{-/-}$ mice infected with *Salmonella* or not. (Data are expressed as mean ± SD; n = 8 mice/group, 2-way ANOVA.) D, Claudin-2 protein expression increased 8.8-fold in VDR$^{-/-}$ mice intestinal epithelial cells and 2.6

hyperreglation of Claudin-2 in intestines lacking VDR regulation. We thus investigated VDR and Claudin-2 in experimental *Salmonella*-colitis mice using $VDR^{-/-}$ and $VDR^{+/-}$ mice (Fig. 2). In the present study, we used $VDR^{+/-}$ mice because we wanted to compare the difference between VDR-null and 1 allele of the VDR gene. Similar results were seen when $VDR^{+/+}$ mice were used (data not shown). $VDR^{-/-}$ mice had more severe infection and lost the integrity of intestinal epithelium post-infection compared with the *Salmonella*-infected $VDR^{+/-}$ mice (Fig. 2A). The inflammation score was significantly higher in the infected $VDR^{-/-}$ mice. Cecum length was smaller in the infected $VDR^{-/-}$ mice compared with the infected $VDR^{+/-}$ mice (Fig. 2B), suggesting more inflammation induced by *Salmonella* in mice lacking VDR. Furthermore, we found that *Salmonella* infected $VDR^{-/-}$ mice had much more body weight loss than $VDR^{+/-}$ mice during day 1 and day 3 post-infection (adjusted P value <0.0001). Compared with $VDR^{+/-}$ and $VDR^{-/-}$ mice, the *Salmonella*-infected mice also significantly dropped more weight than those without the *Salmonella*-infected mice at day 3 (adjusted P value <0.0001) (Fig. 2C). Taken together, our data suggest more severe *Salmonella* infection in the $VDR^{-/-}$ mice.

Uncontrolled Claudin-2 Elevation in $VDR^{-/-}$ Mice with *Salmonella*-Colitis

When performed in vivo, VDR deletion led to reduced Claudin-2 in the basal level of cells without any treatment. After *Salmonella* infection in $VDR^{-/-}$ mice, we observed significantly enhanced Claudin-2 protein by pathogenic *Salmonella* 8 hours post-infection, which is the early stage of infection. The basal levels of claudin-2 protein in $VDR^{-/-}$ organoids and $VDR^{-/-}$ mouse expression are lower compared with $VDR^{+/-}$ organoids and $VDR^{+/-}$ mouse, respectively. After *Salmonella* infection, the similar levels of $VDR^{+/-}$ and $VDR^{-/-}$ Claudin-2 were observed. After normalization to the basal levels accordingly, the fold changes were obtained: *Salmonella* infection induced significant increase of Claudin-2 (Fig. 2D). There was robust increase of Claudin-2 mRNA in inflammatory intestinal epithelial cells that lacked VDR (Fig. 2E).

Vitamin D receptor deletion led to a small amount of Claudin-2 restricted to the crypt base without any treatment. Post-infection, the distribution of Claudin-2 moved from the crypt base to the middle of the crypt in the infected intestine (Fig. 2F). Further, the fluorescence data for intestinal permeability showed that *Salmonella* infection induced higher permeability in both $VDR^{+/-}$ and $VDR^{-/-}$ mice, whereas the $VDR^{-/-}$ mice had significantly high permeability post-infection (Fig. 2G).

Salmonella Translocation in Liver and Spleens of the $VDR^{-/-}$ Mice

We investigated the *Salmonella* load in the intestine and found significantly increased bacterial burden in $VDR^{-/-}$ cecum compared with the $VDR^{+/-}$ mice (Fig. 3A). Bacterial translocation was examined in liver and spleen 4 days post-infection (Fig. 3B and 3C). More *Salmonella* were detected in the liver and spleen of $VDR^{+/-}$ mice, suggesting leaky tight junctions that allow for translocation of gut bacteria to other organs. Culture of *Salmonella* clones further showed that significantly higher numbers of bacterial translocation to liver and spleen of the $VDR^{-/-}$ mice post-*Salmonella* infection compared with the $VDR^{+/-}$ mice (Fig. 3D).

Elevated Level of Intestinal Claudin-2 is Associated With Active Inflammation in $VDR^{-/-}$ Mice

An elevated level of intestinal Claudin-2 is associated with active inflammation.[15,18] We then measured the serum inflammatory cytokines by ELISA (Fig. 3E). We found that Interleukin-6 (IL-6) and tumor necrosis factor alpha (TNF-α) were significantly increased in the infected $VDR^{-/-}$ mice compared with the $VDR^{+/-}$ mice post-infection. We thus hypothesize that inflammation may further drive hyperfunction of Claudin-2 in absence of VDR. Then, we investigated the changes of Claudin-2 in an experimental DSS-induced colitis model. The body weight of the DSS-induced $VDR^{-/-}$ mice dropped more than that of the $VDR^{+/-}$ mice at day 3 (adjusted P value <0.05) (Fig. 4A): 15% body weight loss in $VDR^{-/-}$ mice and 5% body weight loss in $VDR^{+/-}$ mice after DSS treatment for 3 days. We also observed increased intestinal permeability in $VDR^{-/-}$ mice compared with $VDR^{+/-}$ mice 3 days post-DSS (Fig. 4B). In DSS-treated $VDR^{-/-}$ mice, Claudin-2 protein was significantly increased compared with $VDR^{+/-}$ mice treated with DSS. Claudin-2 protein was 5-fold increased in DSS-treated $VDR^{-/-}$ mice compared with the 2-fold increase in $VDR^{+/-}$ mice treated with DSS (Fig. 4C). Location and quantification of Claudin-2 protein in the mouse colons 3 days post-DSS-treatment also confirmed these results (Fig. 4D). Inflammatory cytokines IL-6 and TNF-α are known to increase Claudin-2.[56–58] In the DSS-treated $VDR^{-/-}$ mice, we found significantly higher IL-6 and TNF-α in the serum,

fold in $VDR^{+/-}$ mice intestinal epithelial cells infected with *Salmonella* compared with control. Increased folds of normalized Claudin-2 expressin after *Salmonella* treatment to control. (Data are expressed as mean ± SD; n = 3, Student t test, *P < 0.05). E, Claudin-2 mRNA was upregulated in $VDR^{-/-}$ mice intestinal epithelial cells infected with *Salmonella*. (Data are expressed as mean ± SD; n = 3, 1-way ANOVA test; *P < 0.05). F, Location and quantification of Claudin-2 protein in colons 3 days post-infection with *Salmonella*. Data are from a single experiment and are representative of 5 mice per group. G, Intestine permeability increased in $VDR^{-/-}$ mice infected with *Salmonella*. Mice were treated with *Salmonella* for 3 days. Fluorescein Dextran (Molecular weight 3000 Da, diluted in HBSS) was gavaged (50 mg/g mouse). Four hours later, mouse blood samples were collected for fluorescence intensity measurement. (Data are expressed as mean ± SD; n = 7 mice/group, 1-way ANOVA test; *P < 0.05).

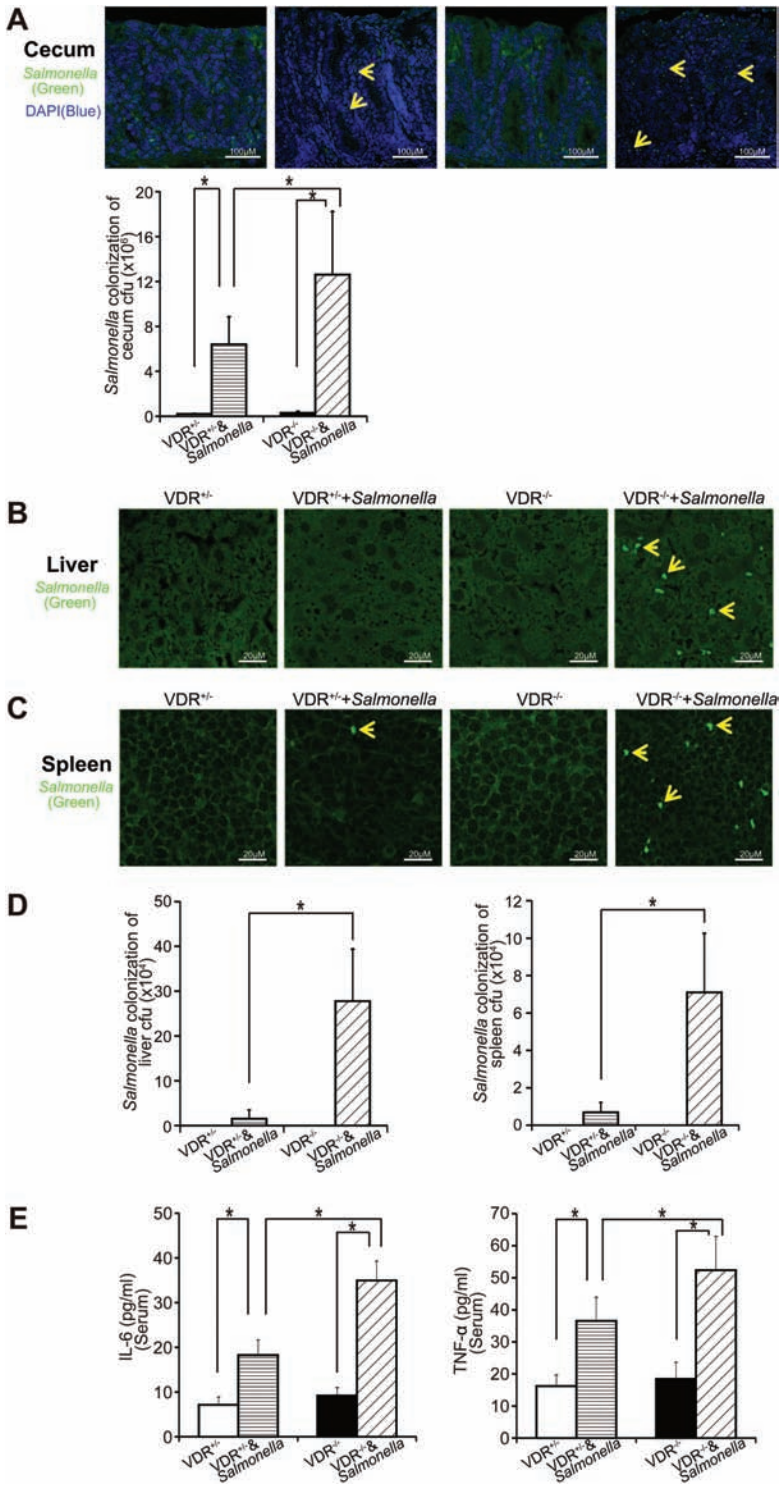

FIGURE 3. Deletion of VDR leads to increased levels of inflammatory cytokines and enhanced *Salmonella* invasion. A, *Salmonella* location and quantification (green) in the ceca of $VDR^{+/-}$ and $VDR^{-/-}$ mice. $VDR^{+/-}$ and $VDR^{-/-}$ mice were infected with *Salmonella* for 3 days. (Data are expressed as mean ± SD; n = 5, 1-way ANOVA test; $^*P < 0.05$). B, *Salmonella* location and quantification (green) in the liver of $VDR^{+/-}$ and $VDR^{-/-}$ mice and C, *Salmonella* location and quantification (green) in the spleen of $VDR^{+/-}$ and $VDR^{-/-}$ mice. $VDR^{+/-}$ and $VDR^{-/-}$ mice were infected with *Salmonella* for 3 days. D, *Salmonella* concentrations in the liver and spleen of $VDR^{-/-}$ mice. Most of *Salmonella* were translocated to the liver and spleen 3 days $VDR^{-/-}$ after being infected with *Salmonella*. (Data are expressed as mean ± SD; n = 5, 1-way ANOVA test; $^*P < 0.05$). E, Serum levels of IL-6 and TNF-α were significantly higher in *Salmonella*-infected $VDR^{-/-}$ mice compared with $VDR^{+/-}$ mice. (Data are expressed as mean ± SD; n = 5, 1-way ANOVA test; $^*P < 0.05$).

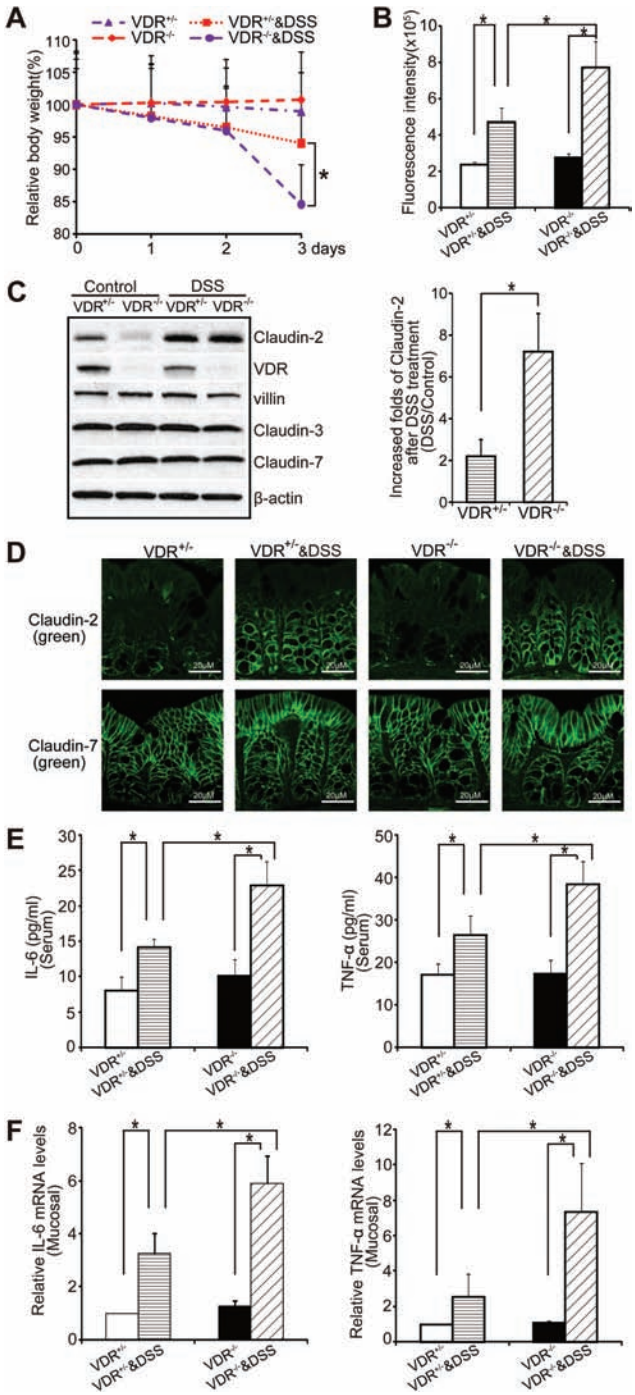

FIGURE 4. Lack of VDR regulation led to increased expression of Claudin-2 protein and inflammatory cytokines IL-6 and TNF-α in the DSS-colitis VDR$^{-/-}$ mice. A, Relative body weight changes in VDR$^{+/-}$ and VDR$^{-/-}$ mice with or without DSS treatment. (Data are expressed as mean ± SD; n = 6 mice/group, 2-way ANOVA). B, DSS increased VDR$^{-/-}$ mice intestine permeability. Mice were treated with DSS for 3 days, and Dextran-3000 was gavaged (50 mg/g mouse). Four hours later, mouse blood samples were collected for fluorescence intensity measurement. (Data are expressed as mean ± SD; n = 6, 1-way ANOVA test; *$P < 0.05$). C, Claudin-2 protein robustly increased in VDR$^{-/-}$ mice intestinal epithelial cells infected with *Salmonella*. Increased folds of internalized Claudin-2 expression after *Salmonella* treatment compared with control. (Data are expressed as mean ± SD; n = 3, Student *t* test; *$P < 0.05$). D, Location and quantification of Claudin-2 protein in colons 3 days post-treatment with DSS. Data are from a single experiment and are representative of 5 mice per group. E, IL-6 and TNF-α in the serum were significantly higher in DSS-treated VDR$^{-/-}$ mice compared with VDR$^{+/-}$ mice. (Data are expressed as mean ± SD; n = 5, 1-way ANOVA test; *$P < 0.05$). F, IL-6 and TNF-α mRNA levels in the intestine were significantly higher in DSS-treated VDR$^{-/-}$ mice compared with VDR$^{+/-}$ mice. (Data are expressed as mean ± SD; n = 5, 1-way ANOVA test; *$P < 0.05$).

as shown in Fig. 4E. In the colonic mucosal samples, we also found higher IL-6 and TNF-α at the mRNA levels (Fig. 4F).

Enhanced Claudin-2 Promoter Activity Through the Binding Sites of NF-κB and STAT

Because VDR is a transcriptional factor, we reason that VDR is the upstream regulator in linking barrier functions in the experimental colitis model and infection. Absence of VDR leads to activation of NF-κB and higher risk of chronic inflammation.[59, 60] We further hypothesize that a robust increase of Claudin-2 in inflamed intestinal epithelial cells may be due to lacking VDR regulation at the transcriptional level, thus allowing the inflammatory cytokines to take over. To study the molecular mechanism of Claudin-2 gene regulation, we mutated the promoter of Claudin-2 at the Cdx, NF-kB, or STAT binding sites (Fig. 5A). In human HCT116 cells, we transfected the plasmid with wild type (WT), ΔNF-kB, ΔSTAT, or ΔCdx, then colonized the cells with *Salmonella*. Our data showed that ΔNF-kB and ΔSTAT led to significantly lower activity of Claudin-2 promoter, whereas ΔCdx did not change the activity of Claudin-2 promoter (Fig. 5B). In CaCO2 cells, we had similar observations (Fig. 5C). Therefore, we identified the enhanced Claudin-2 promoter activity through the binding sites of NF-κB and STAT.

Claudin-2 Protein Expression Was Upregulated in VDR$^{-/-}$ Cells After *Salmonella* Infection Through the NF-κB and STAT3 Pathways

To study the functional regulation for enhanced Claudin-2 through the NF-κB and STAT pathways in the *Salmonella* infection, we treated cells with various inhibitors (Fig. 6). When VDR$^{-/-}$ cells were treated with both NF-κB and STAT3 inhibitors, there was a significant suppression in *Salmonella*-induced Claudin-2 expression in VDR$^{-/-}$ MEF cells, which was also observed in VDR$^{+/-}$ MEF cells colonized with *Salmonella* (Fig. 6A). The NF-κB or STAT3 inhibitors could abolish the enhanced Claudin-2 in *Salmonella*-infectedVDR$^{+/-}$ MEF cells but not in *Salmonella*-infected VDR$^{-/-}$ MEF cells (Fig. S1). *Salmonella*-induced Claudin-2 was suppressed by blocking the stress-activated protein kinase/jun-amino-terminal kinase (SAPK/JNK) pathways.[24] After the treatment of VDR$^{-/-}$ and VDR$^{+/-}$ cells with SAPK/JNK inhibitor, we observed that

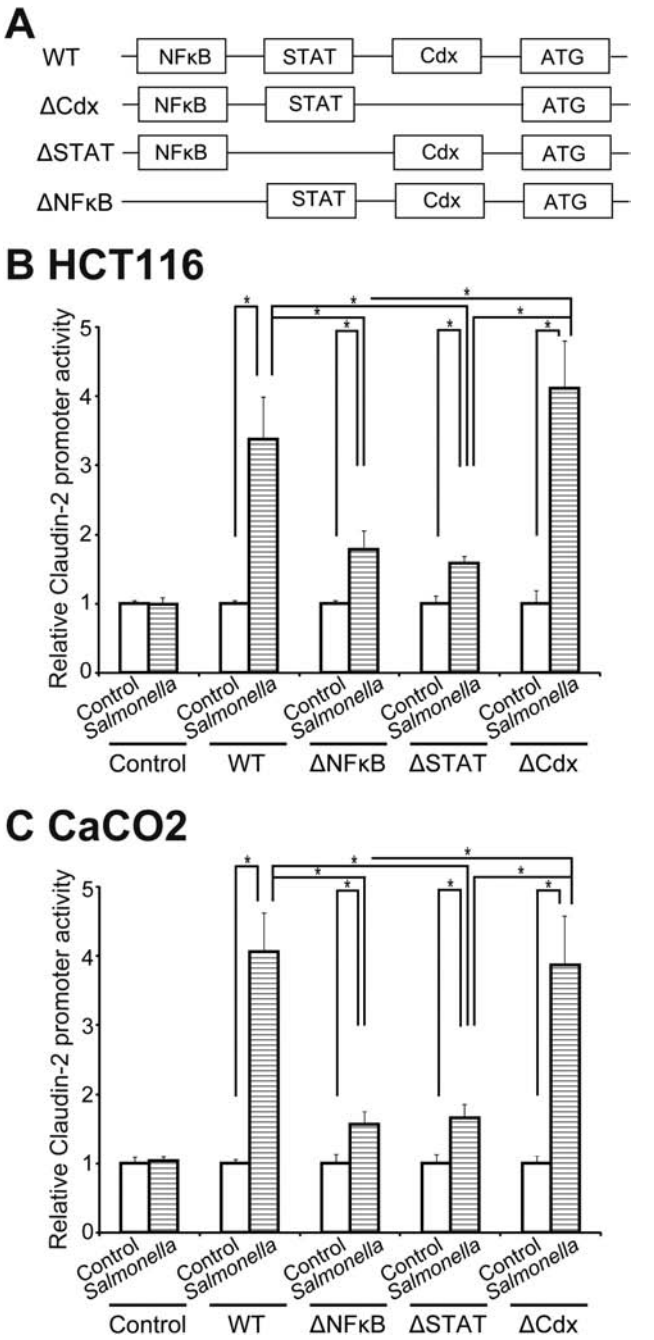

FIGURE 5. *Salmonella* enhanced Claudin-2 promoter activity through the binding sites of NF-κB and STAT. A, A schematic representation of transcriptional binding sites in the WT Claudin-2 promoter and deletion mutants. B, WT or mutant Claudin-2 reporter plasmids were transfected into HCT116 and C, CaCO2 cells and then colonized with *Salmonella*. Luciferase activity was measured in the cell monolayers colonized with *Salmonella* 30 minutes and then incubated with DMEM for 30 minutes. Dual luciferase assays were performed and firefly luciferase activity was normalized to renilla luciferase activity. (Data are expressed as mean ± SD; n = 3, 1-way ANOVA test; *$P < 0.05$).

Salmonella-induced upregulated Claudin-2 expression has been abolished in both VDR$^{+/-}$ and VDR$^{-/-}$ MEF cells (Fig. 6B).

We did coknockdown of VDR and Claudin-2 in intestinal epithelial SKCO15 cells (Fig. S2). We found that the forceful decreased expression of Claudin-2 partly restored the epithelial defects in VDR-depleted epithelial cells infected with *Salmonella*. We also checked p-Iκβα expression, an indicator of NF-κB activation. Western blot data showed that cells with VDR-deficient and reduced expression of Claudin-2 had less p-Iκβα post-infection compared with cells without coknockdown (Fig. S2). These data indicate less inflammatory response to *Salmonella* infection when VDR and Claudin-2 were both reduced.

Reduced VDR Expression Is Associated With Enhanced Claudin-2 in Ulcerative Colitis Patients

In inflamed intestine of ulcerative colitis patients, VDR expression is low (Fig. 7A). We showed that the increased Claudin-2 was associated with the reduction of intestinal VDR in human IBD intestine (Fig. 7B). Our study included 10 normal cases and 16 cases with ulcerative colitis (UC). Compared with normal intestines, UC patients' intestines had a statistically significantly lower VDR and higher Claudin-2 proteins expression (Fig. 7C). We further examined whether cytokines recapitulate the effects of *Salmonella*. The SKCO15 cells were transfected with VDR-siRNA followed by TNF-alpha or IFN-gamma treatment (Fig S3). We found that both TNF-alpha and IFN-gamma could trigger higher Claudin-2 expression in the VDR-deficient epithelial cells.

DISCUSSION

We demonstrate that lack of intestinal VDR leads to hyperfunction of Claudin-2 in inflammatory responses. There was a significant increase of Claudin-2 in inflammatory cells lacking VDR. In a *Salmonella*-colitis model and a DSS-induced colitis model, VDR deletion consequences led to more severe leakage of intestine and inflammation in intestine of VDR$^{-/-}$ mice. Importantly, observation in experimental colitis models was consistent with dysregulation of VDR in inflamed human intestine with robustly increased Claudin-2. Functionally, we find an increase of Claudin-2 in inflammatory intestinal epithelial cells (IECs) lacking VDR. Increased Claudin-2 confers more severe leakage, enhanced permeability, and inflammation in VDR$^{-/-}$ intestine. Inflammatory cytokines in VDR$^{-/-}$ cells further increase Claudin-2 post-infection. Mechanistically, we identified the enhanced Claudin-2 promoter activity through the binding sites of NF-κB and STAT in VDR$^{-/-}$ cells. This study highlights an important mechanism for VDR regulation of Claudin-2 critical to intestinal homeostasis.

Vitamin D receptor target genes include antimicrobial peptide (AMP) cathelicidin precursor (LL-37)[61] and β

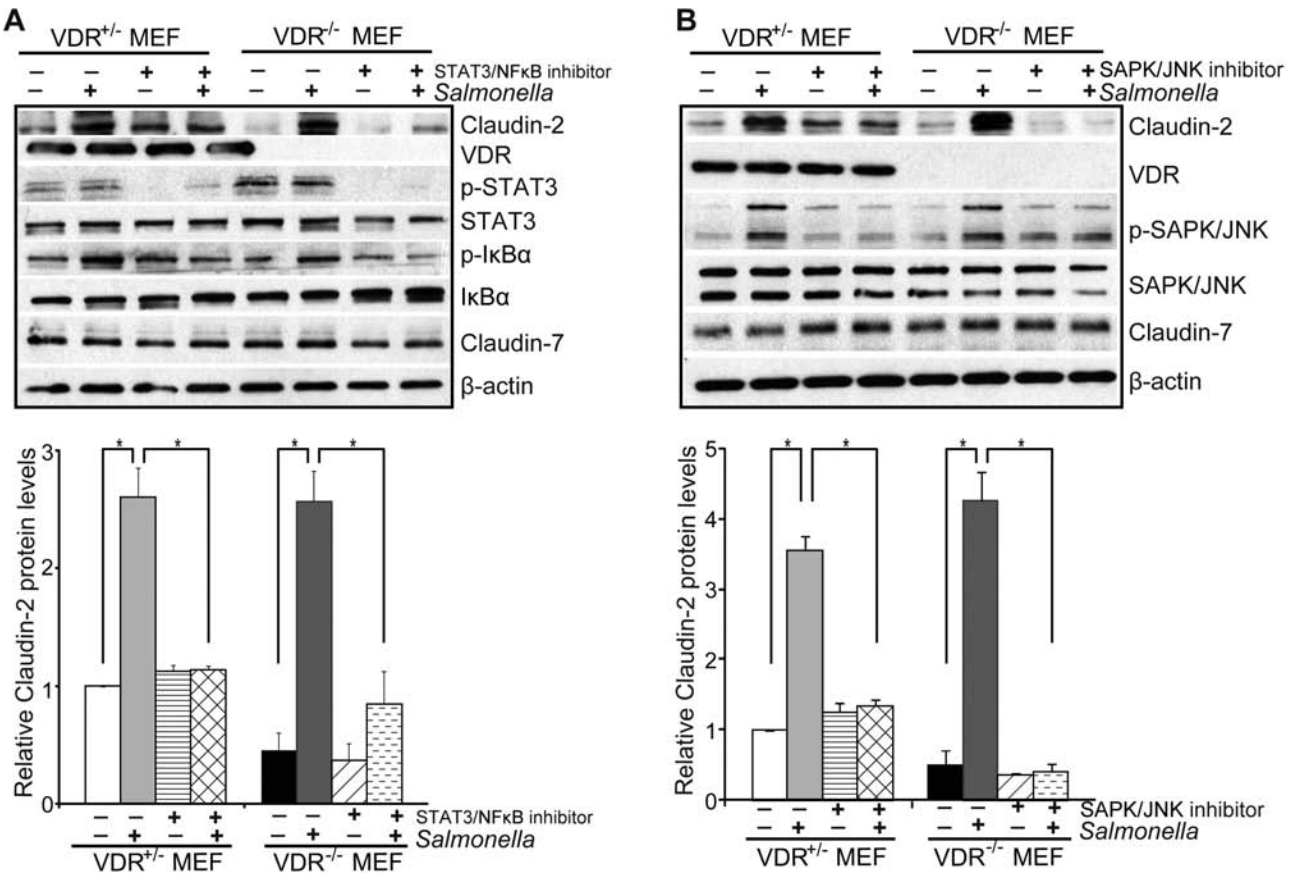

FIGURE 6. Claudin-2 protein expression was up-regulated in *Salmonella*-infected VDR$^{-/-}$ cells in NF-κB and STAT3 pathways. A, Claudin-2 protein expression after *Salmonella* infection can be inhibited by combined NF-κB/STAT3 inhibitors in VDR$^{+/-}$ and VDR$^{-/-}$ MEF cells. MEF cells were first pretreated with 20 μM of stattic and 10 μM of BAY11-7085 for 2 hours, then colonized with *Salmonella* for 30 minutes, then followed by 2-hour incubation of 20 μM of stattic and 10 μM of BAY11-7085. (Data are expressed as mean ± SD; n = 3, 1-way ANOVA test; *$P < 0.05$). B, Claudin-2 protein expression after *Salmonella* infection can be inhibited by SAPK/JNK inhibitor SP600125 in VDR$^{+/-}$ and VDR$^{-/-}$ MEF cells. MEF cells were first pretreated with 50 μM of SP600125 for 1 hour, then colonized with *Salmonella* for 30 minutes, and then incubated for 2 hours of SP600125 at the concentration of 50 μM. (Data are expressed as mean ± SD; n = 3, 1-way ANOVA test; *$P < 0.05$).

defensin.[62] We have identified that Claudin-2[41] and autophagy regulator ATG16L1[26,63] are VDR target genes. We further study the physiological role and mechanism of intestinal epithelial VDR as an upstream regulator of TJs. Here, we showed without any stimulation that Claudin-2 is weak by immunistaining and significantly decreased in colon of VDR$^{-/-}$ mice. However, *Salmonella* infection enhanced Claudin-2 in VDR$^{-/-}$ mice. Claudin-2 staining is significantly enhanced which may explain the observed leaky and bacterial translocation in the *Salmonella*-infected mice. These data suggest that TJs without stimulation may be very different from those with infection. Interestingly, there is no change of Claudin-3 and Claudin-7 in the WT mice and VDR$^{-/-}$ mice with or without *Salmonella* infection, indicating the regulatory role of VDR is selectively on certain junction proteins in intestinal inflamamtion.

The vitamin D receptor has multiple critical functions in regulating innate and adaptive immunity, intestinal homeostasis, host response to invasive pathogens and commensal bacteria, and tight junction structure.[40, 61, 64–70] Severely disrupted TJs and increased permeability were reported in the DSS-treated VDR$^{-/-}$ colonic epithelial cells in vivo.[40] There is a specific regulatory role of VDR on Claudin-2 under both healthy and infectious states. The pathobiological importance of the VDR regulation of Claudin-2 is very interesting. Claudin-2 is enhanced in the inflamed gut in patients with IBD.[15, 18] In the UC-activated inflamed intestine, VDR is low and Claudin-2 is enhanced, suggesting the other regulators that take over and enhance the level of Claudin-2.

We dissected the transcriptional regulation of Claudin-2 under inflamed states in the current study. Based on others' studies and our studies on the promoter of Claudin-2,[4, 16, 56] we know that multiple factors contribute to the upregulation of Claudin-2 at the transcriptional level. TNF-α and IL-1β also contribute to elevated Claudin-2 in vitro.[57, 71] Interleukin-6 enhances Claudin-2 promoter activity in a Cdx-binding, site-dependent manner.[56] Interleukin-22 induces Claudin-2

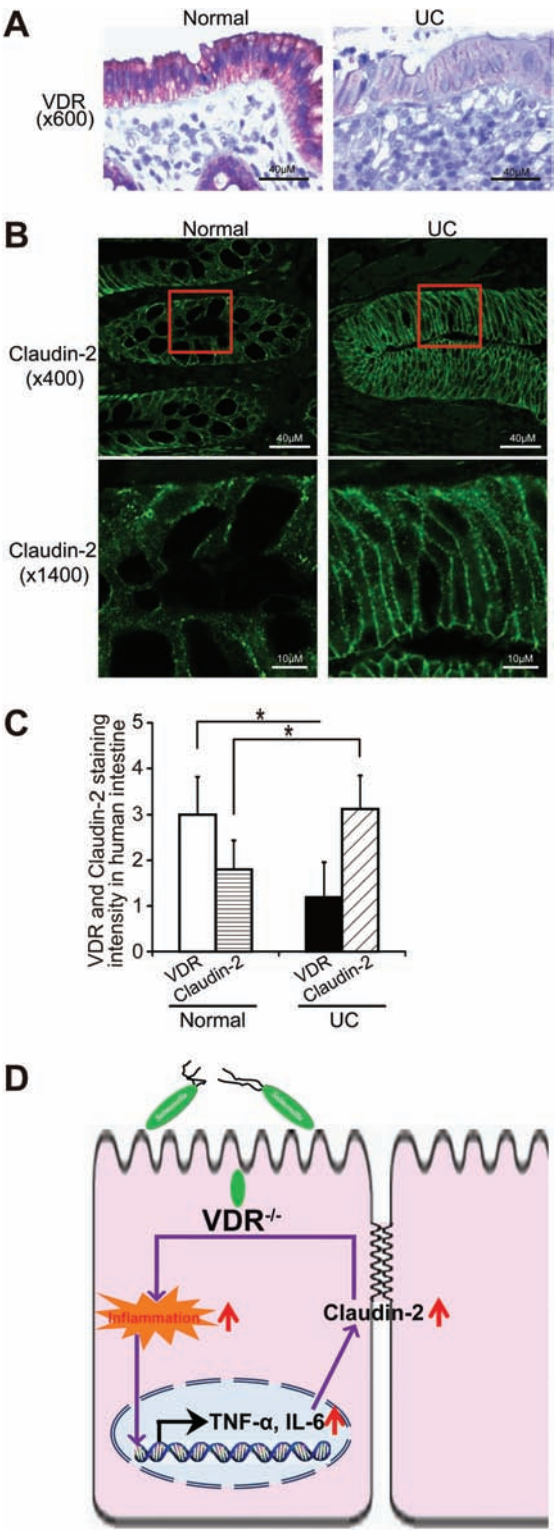

FIGURE 7. Lack of intestinal VDR led to hyperfunction of Claudin-2 in inflammatory responses. A, VDR IHC staining in normal and UC human colon. Images were representative of experiments that we carried out in triplicates (normal, n = 10; UC, n = 16). B, Claudin-2 staining in normal and UC human colon. Images were representative of experiments that we carried out in triplicates (normal, n = 10; UC, n = 16). C, Compared with normal intestines, UC patients' intestines had a statistically significantly lower VDR and higher Claudin-2 proteins expression. (Data are expressed as mean ± SD; normal, n = 10; UC, n = 16; Student *t* tes; **P* < 0.05). D, A working model of VDR in intestinal inflammation and tight junctions. In inflamed intestine of ulcerative colitis patients, VDR expression was low and Claudin-2 was high. Inflammatory cytokines (eg, IL-6 and TNF-α), induced by bacterial infection and chronic inflammation, were significantly higher in the intestine. These cytokines take over to further enhance Claudin-2 in absence of VDR.

upregulation to drive diarrhea and pathogen clearance.[72] Recent evidence also suggests that Claudin-2 is relevant to neoplastic transformation and growth via epidermal growth factor receptor (EGFR) transactivation.[73] Absence of VDR in the intestine leads to activation of NF-κB and higher risk of chronic inflammation.[59, 60] Our study has demonstrated that we need to inhibit both NF-kB and STAT3 promoters to abolish the *Salmonella*-induced inflammation in the VDR$^{-/-}$ cells. Thus, chronic inflammation enhances the expression of Claudin-2.

In the current study, the regulatory role of intestinal VDR has not been studied in the tissue-specific knockout mouse models. We only investigated the samples from UC patients, not Crohn's disease patients. We plan to study both UC and CD samples in the future. Intestinal permeability and inflammation are regulated by various proteins (eg, Junctional Adhesion Molecule [JAM-A] and myosin IIA).[48, 74] It will be very interesting to identify other regulators that modulate the level of Claudin-2 and tissue barriers in inflamed VDR-deficient tissues in human IBD.

In summary, our study provides new insights into VDR on TJs in infected and inflamed intestine. Lacking VDR may lead to the hyperfunction of Claudin-2 and increase permeability in the inflammatory state, as we see in the murine colitis models and human IBD samples (Fig. 7D). Our studies highlight the complex role of VDR in bacterial infection and chronic inflammation.[71, 75] It will provide ideas for developing new therapeutic targets by enhancing function of intestinal epithelial VDR for alleviating infection and chronic inflammation.

SUPPLEMENTARY DATA

Supplementary data is available at *Inflammatory Bowel Diseases* online.

ACKNOWLEDGEMENTS

The authors thank Dr. Takuya Suzuki from Hiroshima University, Japan, for generously providing the Claudin-2 reporter plasmids. They would like to acknowledge the NIDDK/National Institutes of Health grant R01 DK105118, R01DK114126, and DOD BC160450P1 to JS.

REFERENCES

1. Su L, Shen L, Clayburgh DR, et al. Targeted epithelial tight junction dysfunction causes immune activation and contributes to development of experimental colitis. *Gastroenterology.* 2009;136:551–563.

2. Al-Sadi R, Khatib K, Guo S, et al. Occludin regulates macromolecule flux across the intestinal epithelial tight junction barrier. *Am J Physiol Gastrointest Liver Physiol.* 2011;300:G1054–G1064.
3. Rahner C, Mitic LL, Anderson JM. Heterogeneity in expression and subcellular localization of claudins 2, 3, 4, and 5 in the rat liver, pancreas, and gut. *Gastroenterology.* 2001;120:411–422.
4. Sakaguchi T, Gu X, Golden HM, et al. Cloning of the human claudin-2 5'-flanking region revealed a TATA-less promoter with conserved binding sites in mouse and human for caudal-related homeodomain proteins and hepatocyte nuclear factor-1alpha. *J Biol Chem.* 2002;277:21361–21370.
5. McCole DF. IBD candidate genes and intestinal barrier regulation. *Inflamm Bowel Dis.* 2014;20:1829–1849.
6. Anderson JM, Van Itallie CM. Physiology and function of the tight junction. *Cold Spring Harb Perspect Biol.* 2009;1:a002584.
7. Schulzke JD, Ploeger S, Amasheh M, et al. Epithelial tight junctions in intestinal inflammation. *Ann N Y Acad Sci.* 2009;1165:294–300.
8. Rosenthal R, Günzel D, Theune D, et al. Water channels and barriers formed by claudins. *Ann N Y Acad Sci.* 2017;1397:100–109.
9. Escaffit F, Boudreau F, Beaulieu JF. Differential expression of claudin-2 along the human intestine: implication of GATA-4 in the maintenance of claudin-2 in differentiating cells. *J Cell Physiol.* 2005;203:15–26.
10. Holmes JL, Van Itallie CM, Rasmussen JE, et al. Claudin profiling in the mouse during postnatal intestinal development and along the gastrointestinal tract reveals complex expression patterns. *Gene Expr Patterns.* 2006;6:581–588.
11. Furuse M. Molecular basis of the core structure of tight junctions. *Cold Spring Harb Perspect Biol.* 2010;2:a002907.
12. Amasheh S, Meiri N, Gitter AH, et al. Claudin-2 expression induces cation-selective channels in tight junctions of epithelial cells. *J Cell Sci.* 2002;115:4969–4976.
13. Colegio OR, Van Itallie CM, McCrea HJ, et al. Claudins create charge-selective channels in the paracellular pathway between epithelial cells. *Am J Physiol Cell Physiol.* 2002;283:C142–C147.
14. Van Itallie CM, Anderson JM. Claudins and epithelial paracellular transport. *Annu Rev Physiol.* 2006;68:403–429.
15. Zeissig S, Bürgel N, Günzel D, et al. Changes in expression and distribution of Claudin-2, 5 and 8 lead to discontinuous tight junctions and barrier dysfunction in active Crohn's disease. *Gut.* 2007;56:61–72.
16. Rosenthal R, Milatz S, Krug SM, et al. Claudin-2, a component of the tight junction, forms a paracellular water channel. *J Cell Sci.* 2010;123:1913–1921.
17. Van Itallie CM, Holmes J, Bridges A, et al. Claudin-2-dependent changes in noncharged solute flux are mediated by the extracellular domains and require attachment to the PDZ-scaffold. *Ann N Y Acad Sci.* 2009;1165:82–87.
18. Weber CR, Nalle SC, Tretiakova M, et al. Claudin-1 and claudin-2 expression is elevated in inflammatory bowel disease and may contribute to early neoplastic transformation. *Lab Invest.* 2008;88:1110–1120.
19. Luettig J, Rosenthal R, Barmeyer C, et al. Claudin-2 as a mediator of leaky gut barrier during intestinal inflammation. *Tissue Barriers.* 2015;3:e977176.
20. Mahapatro M, Foersch S, Hefele M, et al. Programming of intestinal epithelial differentiation by IL-33 derived from pericryptal fibroblasts in response to systemic infection. *Cell Rep.* 2016;15:1743–1756.
21. Schultz BM, Paduro CA, Salazar GA, et al. A potential role of salmonella infection in the onset of inflammatory bowel diseases. *Front Immunol.* 2017;8:191.
22. Lin Z, Zhang YG, Xia Y, et al. Salmonella enteritidis effector avra stabilizes intestinal tight junctions via the JNK pathway. *J Biol Chem.* 2016;291:26837–26849.
23. Liao AP, Petrof EO, Kuppireddi S, et al. Salmonella type III effector avra stabilizes cell tight junctions to inhibit inflammation in intestinal epithelial cells. *Plos One.* 2008;3:e2369.
24. Zhang YG, Wu S, Xia Y, et al. Salmonella infection upregulates the leaky protein claudin-2 in intestinal epithelial cells. *Plos One.* 2013;8:e58606.
25. Demay MB. Mechanism of vitamin D receptor action. *Ann N Y Acad Sci.* 2006;1068:204–213.
26. Wu S, Zhang YG, Lu R, et al. Intestinal epithelial vitamin D receptor deletion leads to defective autophagy in colitis. *Gut*. 2015;64:1082–1094.
27. Bakke D, Sun J. Ancient nuclear receptor VDR with new functions: microbiome and inflammation. *Inflamm Bowel Dis.* 2018;24:1149–1154.
28. Sentongo TA, Semaeo EJ, Stettler N, et al. Vitamin D status in children, adolescents, and young adults with Crohn disease. *Am J Clin Nutr.* 2002;76:1077–1081.
29. Abreu MT, Kantorovich V, Vasiliauskas EA, et al. Measurement of vitamin D levels in inflammatory bowel disease patients reveals a subset of Crohn's disease patients with elevated 1,25-dihydroxyvitamin D and low bone mineral density. *Gut.* 2004;53:1129–1136.
30. Lim WC, Hanauer SB, Li YC. Mechanisms of disease: vitamin D and inflammatory bowel disease. *Nat Clin Pract Gastroenterol Hepatol.* 2005;2:308–315.
31. Wang TT, Dabbas B, Laperriere D, et al. Direct and indirect induction by 1,25-dihydroxyvitamin D3 of the NOD2/CARD15-defensin beta2 innate immune pathway defective in Crohn disease. *J Biol Chem.* 2010;285:2227–2231.
32. Rufo PA, Bousvaros A. Current therapy of inflammatory bowel disease in children. *Paediatr Drugs.* 2006;8:279–302.
33. Simmons JD, Mullighan C, Welsh KI, et al. Vitamin D receptor gene polymorphism: association with Crohn's disease susceptibility. *Gut* 2000;47:211–4.
34. Pei FH, Wang YJ, Gao SL, et al. Vitamin D receptor gene polymorphism and ulcerative colitis susceptibility in han chinese. *J Dig Dis.* 2011;12:90–98.
35. Naderi N, Farnood A, Habibi M, et al. Association of vitamin D receptor gene polymorphisms in iranian patients with inflammatory bowel disease. *J Gastroenterol Hepatol.* 2008;23:1816–1822.
36. Kim JH, Yamaori S, Tanabe T, et al. Implication of intestinal VDR deficiency in inflammatory bowel disease. *Biochim Biophys Acta.* 2013;1830:2118–2128.
37. Hughes DJ, McManus R, Neary P, et al. Common variation in the vitamin D receptor gene and risk of inflammatory bowel disease in an irish case-control study. *Eur J Gastroenterol Hepatol.* 2011;23:807–812.
38. Chiba H, Osanai M, Murata M, et al. Transmembrane proteins of tight junctions. *Biochim Biophys Acta.* 2008;1778:588–600.
39. Fujita H, Sugimoto K, Inatomi S, et al. Tight junction proteins claudin-2 and -12 are critical for vitamin D-dependent ca2+ absorption between enterocytes. *Mol Biol Cell.* 2008;19:1912–1921.
40. Kong J, Zhang Z, Musch MW, et al. Novel role of the vitamin D receptor in maintaining the integrity of the intestinal mucosal barrier. *Am J Physiol Gastrointest Liver Physiol.* 2008;294:G208–G216.
41. Zhang YG, Wu S, Lu R, et al. Tight junction CLDN2 gene is a direct target of the vitamin D receptor. *Sci Rep.* 2015;5:10642.
42. Wang TT, Tavera-Mendoza LE, Laperriere D, et al. Large-scale in silico and microarray-based identification of direct 1,25-dihydroxyvitamin D3 target genes. *Mol Endocrinol.* 2005;19:2685–2695.
43. Van Cromphaut SJ, Dewerchin M, Hoenderop JG, et al. Duodenal calcium absorption in vitamin D receptor-knockout mice: functional and molecular aspects. *Proc Natl Acad Sci U S A.* 2001;98:13324–13329.
44. Zhang YG, Wu S, Xia Y, et al. Salmonella-infected crypt-derived intestinal organoid culture system for host-bacterial interactions. *Physiol Rep.* 2014;2:doi:10.14814/phy2.12147.
45. Lu R, Voigt RM, Zhang Y, et al. Alcohol injury damages intestinal stem cells. *Alcohol Clin Exp Res.* 2017;41:727–734.
46. Sun J, Hobert ME, Rao AS, et al. Bacterial activation of beta-catenin signaling in human epithelia. *Am J Physiol Gastrointest Liver Physiol.* 2004;287:G220–G227.
47. Wu S, Lu R, Zhang YG, et al. Chronic Salmonella infected mouse model. *J Vis Exp.* 2010.
48. Laukoetter MG, Nava P, Lee WY, et al. JAM-A regulates permeability and inflammation in the intestine in vivo. *J Exp Med.* 2007;204:3067–3076.
49. Barthel M, Hapfelmeier S, Quintanilla-Martínez L, et al. Pretreatment of mice with streptomycin provides a *Salmonella* enterica serovar typhimurium colitis model that allows analysis of both pathogen and host. *Infect Immun.* 2003;71:2839–2858.
50. Dieleman LA, Palmen MJ, Akol H, et al. Chronic experimental colitis induced by dextran sulphate sodium (DSS) is characterized by th1 and th2 cytokines. *Clin Exp Immunol.* 1998;114:385–391.
51. Duan Y, Liao AP, Kuppireddi S, et al. Beta-catenin activity negatively regulates bacteria-induced inflammation. *Lab Invest.* 2007;87:613–624.
52. Sun J, Hobert ME, Duan Y, et al. Crosstalk between NF-kappab and beta-catenin pathways in bacterial-colonized intestinal epithelial cells. *Am J Physiol Gastrointest Liver Physiol.* 2005;289:G129–G137.
53. Lu R, Wu S, Liu X, et al. Chronic effects of a salmonella type III secretion effector protein avra in vivo. *Plos One.* 2010;5:e10505.
54. Lu R, Bosland M, Xia Y, et al. Presence of salmonella avra in colorectal tumor and its precursor lesions in mouse intestine and human specimens. *Oncotarget.* 2017;8:55104–55115.
55. Zhang YG, Wu S, Xia Y, et al. Salmonella-infected crypt-derived intestinal organoid culture system for host-bacterial interactions. *Physiol. Rep.* 2014;2. doi:10.14814/phy2.12147.
56. Suzuki T, Yoshinaga N, Tanabe S. Interleukin-6 (IL-6) regulates claudin-2 expression and tight junction permeability in intestinal epithelium. *J Biol Chem.* 2011;286:31263–31271.
57. Mankertz J, Amasheh M, Krug SM, et al. Tnfalpha up-regulates claudin-2 expression in epithelial HT-29/B6 cells via phosphatidylinositol-3-kinase signaling. *Cell Tissue Res.* 2009;336:67–77.
58. Al-Sadi R, Ye D, Boivin M, et al. Interleukin-6 modulation of intestinal epithelial tight junction permeability is mediated by JNK pathway activation of claudin-2 gene. *Plos One.* 2014;9:e85345.
59. Wu S, Liao AP, Xia Y, et al. Vitamin D receptor negatively regulates bacterial-stimulated NF-kappab activity in intestine. *Am J Pathol.* 2010;177:686–697.
60. Sun J, Mustafi R, Cerda S, et al. Lithocholic acid down-regulation of NF-kappab activity through vitamin D receptor in colonic cancer cells. *J Steroid Biochem Mol Biol.* 2008;111:37–40.
61. Gombart AF, Borregaard N, Koeffler HP. Human cathelicidin antimicrobial peptide (CAMP) gene is a direct target of the vitamin D receptor and is strongly up-regulated in myeloid cells by 1,25-dihydroxyvitamin D3. *Faseb J.* 2005;19:1067–1077.

62. Wang TT, Nestel FP, Bourdeau V, et al. Cutting edge: 1,25-dihydroxyvitamin D3 is a direct inducer of antimicrobial peptide gene expression. *J Immunol.* 2004;173:2909–2912.
63. Sun J. Vitamin D receptor regulates autophagic activity through ATG16L1. *Autophagy.* 2016;12:1057–1058.
64. Ogura M, Nishida S, Ishizawa M, et al. Vitamin D3 modulates the expression of bile acid regulatory genes and represses inflammation in bile duct-ligated mice. *J Pharmacol Exp Ther.* 2009;328:564–570.
65. Kamen DL, Tangpricha V. Vitamin D and molecular actions on the immune system: modulation of innate and autoimmunity. *J Mol Med (Berl).* 2010;88:441–450.
66. Waterhouse JC, Perez TH, Albert PJ. Reversing bacteria-induced vitamin D receptor dysfunction is key to autoimmune disease. *Ann N Y Acad Sci.* 2009;1173:757–765.
67. Liu PT, Krutzik SR, Modlin RL. Therapeutic implications of the TLR and VDR partnership. *Trends Mol Med.* 2007;13:117–124.
68. Lagishetty V, Misharin AV, Liu NQ, et al. Vitamin D deficiency in mice impairs colonic antibacterial activity and predisposes to colitis. *Endocrinology.* 2010;151:2423–2432.
69. Adams JS, Hewison M. Unexpected actions of vitamin D: new perspectives on the regulation of innate and adaptive immunity. *Nat Clin Pract Endocrinol Metab.* 2008;4:80–90.
70. Yu S, Bruce D, Froicu M, et al. Failure of T cell homing, reduced CD4/CD8ALPHAALPHA intraepithelial lymphocytes, and inflammation in the gut of vitamin D receptor KO mice. *Proc Natl Acad Sci U S A.* 2008;105:20834–20839.
71. Yamamoto T, Kojima T, Murata M, et al. IL-1beta regulates expression of cx32, occludin, and claudin-2 of rat hepatocytes via distinct signal transduction pathways. *Exp Cell Res.* 2004;299:427–441.
72. Tsai PY, Zhang B, He WQ, et al. IL-22 upregulates epithelial claudin-2 to drive diarrhea and enteric pathogen clearance. *Cell Host Microbe.* 2017;21:671–681.e4.
73. Dhawan P, Ahmad R, Chaturvedi R, et al. Claudin-2 expression increases tumorigenicity of colon cancer cells: role of epidermal growth factor receptor activation. *Oncogene.* 2011;30:3234–3247.
74. Naydenov NG, Feygin A, Wang D, et al. Nonmuscle myosin IIA regulates intestinal epithelial barrier in vivo and plays a protective role during experimental colitis. *Sci Rep.* 2016;6:24161.
75. Zhang YG, Wu S, Sun J. Vitamin D, vitamin D receptor, and tissue barriers. *Tissue Barriers.* 2013;1:e23118.